JARO 20: 449–459 (2019)
DOI: 10.1007/s10162-019-00727-1

JARO
Journal of the Association for Research in Otolaryngology

Research Article

Osteoclasts Modulate Bone Erosion in Cholesteatoma via RANKL Signaling

Ryusuke Imai,[1] Takashi Sato,[1] Yoriko Iwamoto,[1] Yukiko Hanada,[1] Mika Terao,[2] Yumi Ohta,[1] Yasuhiro Osaki,[1] Takao Imai,[1] Tetsuo Morihana,[3] Suzuyo Okazaki,[4] Kazuo Oshima,[1] Daisuke Okuzaki,[5] Ichiro Katayama,[2] and Hidenori Inohara[1]

[1]*Department of Otorhinolaryngology-Head and Neck Surgery, Osaka University Graduate School of Medicine, 2-2, Yamadaoka, Suita, Osaka, 565-0871, Japan*

[2]*Department of Dermatology, Osaka University Graduate School of Medicine, 2-2 Yamadaoka, Suita, Osaka, 565-0871, Japan*

[3]*Department of Otorhinolaryngology-Head and Neck Surgery, Higashiosaka City Medical Center, 3-4-5 Nishiiwata, Higashiosaka, Osaka, 578-8588, Japan*

[4]*Department of Otorhinolaryngology, Osaka City General Hospital, 2-13-22 Miyakojimahondori, Miyakojimaku, Osaka, 534-0021, Japan*

[5]*Genome Information Research Center, Research Institute for Microbial Diseases, Osaka University, 3-1 Yamadaoka, Suita, Osaka, 565-0871, Japan*

Received: 3 April 2019; Accepted: 21 May 2019; Online publication: 28 June 2019

ABSTRACT

Cholesteatoma starts as a retraction of the tympanic membrane and expands into the middle ear, eroding the surrounding bone and causing hearing loss and other serious complications such as brain abscess and meningitis. Currently, the only effective treatment is complete surgical removal, but the recurrence rate is relatively high. In rheumatoid arthritis (RA), osteoclasts are known to be responsible for bone erosion and undergo differentiation and activation by receptor activator of NF-κB ligand (RANKL), which is secreted by synovial fibroblasts, T cells, and B cells. On the other hand, the mechanism of bone erosion in cholesteatoma is still controversial. In this study, we found that a significantly larger number of osteoclasts were observed on the eroded bone adjacent to cholesteatomas than in unaffected areas, and that fibroblasts in the cholesteatoma perimatrix expressed RANKL. We also investigated upstream transcription factors of RANKL using RNA sequencing results obtained via Ingenuity Pathways Analysis, a tool that identifies relevant targets in molecular biology systems. The concentrations of four candidate factors, namely interleukin-1β, interleukin-6, tumor necrosis factor α, and prostaglandin E2, were increased in cholesteatomas compared with normal skin. Furthermore, *interleukin-1β* was expressed in infiltrating inflammatory cells in the cholesteatoma perimatrix. This is the first report demonstrating that a larger-than-normal number of osteoclasts are present in cholesteatoma, and that the disease involves upregulation of factors related to osteoclast activation. Our study elucidates the molecular basis underlying bone erosion in cholesteatoma.

Keywords: cholesteatoma, osteoclast, fibroblast, receptor activator of NF-κB ligand (RANKL), RNA sequencing, IL-1β

INTRODUCTION

Cholesteatoma, a chronic ear disease that causes hearing loss and ear discharge, is a squamous

Electronic supplementary material The online version of this article (https://doi.org/10.1007/s10162-019-00727-1) contains supplementary material, which is available to authorized users.

Correspondence to: Takashi Sato · Department of Otorhinolaryngology-Head and Neck Surgery · Osaka University Graduate School of Medicine · 2-2, Yamadaoka, Suita, Osaka, 565-0871, Japan. Telephone: +81-6-6879-3951; email: tsato@ent.med.osaka-u.ac.jp

epithelial lesion that arises from a portion of the tympanic membrane and expands into the middle ear as a cyst or pouch. It consists of three components: the matrix, perimatrix, and cystic content (Kuo et al. 2015). The matrix is composed of keratinizing stratified squamous epithelium. The perimatrix surrounds the matrix and contains collagen fibers, fibroblasts, and inflammatory cells. The cystic content is the most internal component and consists of keratin debris and necrotic tissues. Cholesteatoma is characterized by both overgrowth of keratinized squamous epithelium and bone erosion in the middle ear (Chen et al. 2015; Olszewska et al. 2004), and it eventually causes various complications such as conductive and/or sensorineural hearing loss, vestibular dysfunction, facial nerve palsy, and fatal intracranial complications, i.e., brain abscess and meningitis. The only effective treatment is complete surgical excision, but the postoperative recurrence rate remains unsatisfactory (Tomlin et al. 2013).

Although the pathogenesis of cholesteatoma has been studied and discussed for a long time, the mechanism of the associated bone resorption remains unclear. Osteoclast activation (Chole 1984; Hamzei et al. 2003; Si et al. 2015), pressure necrosis (Abramson et al. 1984; Huang et al. 1990), acid lysis (Iino et al. 1983; Koizumi et al. 2015), enzymatic mediators (Jung et al. 2004; Kobayashi et al. 2005), inflammatory mediators (Cheshire et al. 1991; Chi et al. 2015; Kuczkowski et al. 2011; Si et al. 2015), and combinations of two or more of these mechanisms have been proposed thus far.

Whether or not osteoclasts are present in cholesteatoma has been controversial. Although morphological studies used light or electron microscopy to demonstrate the presence of osteoclasts on bone surfaces around cholesteatoma lesions (Chole 1984; Si et al. 2015; Uno and Saito 1995), they did not compare the number of osteoclasts in control areas. Bone remodeling is characterized by a balance between bone resorption by osteoclasts and bone formation by osteoblasts (Takayanagi 2007). When this balance tilts to either side, various skeletal disorders may occur. Since osteoclasts exist to some extent even on normal (non-inflammatory) bone surfaces, so as to maintain bone homeostasis, in disease states, it is crucial to compare lesional and non-lesional regions. Of note, the absence of osteoclasts in cholesteatoma has also been reported (Koizumi et al. 2017).

Osteoclasts are multinuclear and differentiate from monocyte-lineage hematopoietic precursor cells (Boyle et al. 2003). The differentiation and activation of osteoclasts are regulated by macrophage colony-stimulating factor (M-CSF) and receptor activator of nuclear factor κB ligand (RANKL) (Teitelbaum and Ross 2003). Overproduction of RANKL is implicated in a variety of degenerative bone diseases, such as rheumatoid arthritis (RA) (Kim et al. 2007; Takayanagi et al. 2000) and periodontitis (Cochran 2008; Fujihara et al. 2014). In these disorders, the major sources of RANKL are proposed to be fibroblast-like synoviocytes or immune cells such as T lymphocytes and macrophages that infiltrate into the lesional area (McInnes and Schett 2011). In patients with RA, macrophages and T helper 17 (Th17) cells express proinflammatory cytokines such as tumor necrosis factor α (TNF-α), interleukin-1 (IL-1), and interleukin-6 (IL-6) (Sato et al. 2006), which stimulate synoviocytes to express RANKL (Kim et al. 2007). Likewise, inflammation has been confirmed to be essential for cholesteatoma formation, growth, and expansion, including the bone resorption process (Likus et al. 2016; Peek et al. 2003; Xie et al. 2016; Yetiser et al. 2002). IL-1, IL-6, TNF-α, and prostaglandin E2 (PGE2) have been investigated as inflammatory mediators of cholesteatoma progression. They are assumed to enhance bone resorption by activating osteoclasts (Jung and Juhn 1988; Kuczkowski et al. 2011; Vitale and Ribeiro Fde 2007). Si et al. (Si et al. 2015) reported that toll-like receptor-4 (TLR-4) signaling induced inflammatory mediators in cholesteatoma and caused bone resorption. On the other hand, it is still unclear whether osteoclasts are involved in the bone destruction caused by cholesteatoma, whether an increased number of osteoclasts are present on the bone surface, and what intercellular communications activate and differentiate osteoclasts.

The objectives of the current study were to investigate whether osteoclasts proliferated on the bone surface adjacent to cholesteatoma, to examine whether the microenvironment in the cholesteatoma perimatrix is suitable for differentiation and activation of osteoclasts, and to propose candidate upstream transcription factors for stimulating osteoclastogenesis in cholesteatoma using thorough computer analyses.

MATERIALS AND METHODS

Patients and Tissue Samples

Twenty-four cholesteatoma specimens from 24 patients who underwent tympanomastoidectomy were examined in the current study. The specimens were collected along with the surrounding eroded bone. The temporal mastoid bone and retroauricular skin at the incision site were also collected as controls. Since there is no tissue in the middle ear that has the same structure as cholesteatomas, we adopted the retroauricular skin as the best control for cholesteatoma. The current study was approved by the ethics committee of Osaka University Hospital (No. 135543).

Histological Techniques

The specimens for histological analyses were fixed in 4 % paraformaldehyde (PFA) overnight, and then bone-connected cholesteatomas and control bones were decalcified for 7 days in 10 % ethylene diamine tetra-acetic acid (EDTA) diluted in 0.1 M phosphate buffer (pH 7.4). These samples were embedded in paraffin. For pathological observation, deparaffinized sections at a thickness of 3 μm were stained with hematoxylin and eosin.

Tartrate-Resistant Acid Phosphatase Staining and Osteoclast Counting

Osteoclasts were stained using tartrate-resistant acid phosphatase (TRAP)-hematoxylin counterstaining. Samples were cut into 5-μm-thick sections and TRAP stained with a TRAP Staining kit (Cosmo, Tokyo, Japan). Briefly, the sections were deparaffinized using xylene and ethanol, rinsed in running distilled water for 5 min, incubated in 100 μl of staining solution at room temperature for 30 min, and then rinsed in distilled water. Following counterstaining in hematoxylin, they were washed in running water for 5 min and dehydrated on a 37 °C heat plate. They were then dropped into xylene and mounted with HSR solution.

Osteoclasts were defined by positive TRAP staining and multiple nuclei, and by their location on the surface of the bone (Ritchlin et al. 2003). The number of osteoclasts was counted as reported previously (Rehman et al. 1994). In the current study, osteoclast numbers were normalized by cross-sectional bone areas that were measured by Adobe Photoshop CC software (Adobe, San Jose, CA).

RNA Isolation and Droplet Digital Polymerase Chain Reaction

Total RNAs and cDNAs were prepared using an RNeasy® Fibrous Tissue Mini Kit (Qiagen) and ReverTra Ace® (Toyobo, Osaka, Japan). To quantify *RANKL* mRNAs, ddPCR was performed on the QX200 droplet digital polymerase chain reaction (ddPCR) system (Bio-Rad, Hercules, CA) using TaqMan® FAM-labeled probes for *RANKL* and HEX-labeled probes for *glyceraldehyde-3-phosphate dehydrogenase* (*GAPDH*) as an endogenous control (Bio-Rad). The absolute copy number of transcripts in reaction samples was measured using Quanta Software version 1.7.4 (Bio-Rad).

Diaminobenzidine Staining and Double Immunofluorescent Staining

Deparaffinized sections at a thickness of 3 μm were blocked with Protein Block (Dako, CA) for 30 min after antigen retrieval for 10 min in Tris-EDTA (pH 9.0) in a 120 °C oil bath. For diaminobenzidine (DAB) staining, endogenous peroxidase activity was quenched with 0.3 % H_2O_2 for 30 min. Sections were then stained overnight at 4 °C with anti-RANKL antibody (rabbit polyclonal IgG, 1:100, Abcam, Cambridge, United Kingdom). A Vectastain® elite ABC kit and the protocol provided by the manufacturer were used. Sections were counterstained with hematoxylin for 30 s before mounting with Paramount-N (Falma, Japan). Normal rabbit IgG was used as the isotype control. For double immunofluorescent staining, sections were then incubated with anti-RANKL antibody (rabbit polyclonal IgG, 1:100, Abcam, Cambridge, UK) and anti-vimentin antibody (mouse monoclonal IgG1, no dilution, Dako, CA) overnight at 4 °C. Instead of anti-RANKL antibody, normal rabbit IgG was used as an isotype control for RANKL protein detection. The sections were washed in phosphate-buffered saline (PBS) following each incubation. Subsequently, the sections were incubated with Alexa Fluor® 555-conjugated goat anti-rabbit IgG (1:500, Invitrogen), Alexa Fluor® 488-conjugated goat anti-mouse IgG (1:500, Invitrogen), and Hoechst® 33,342 (1:1000, Molecular Probes, OR) at room temperature for 1 h. After rinsing with PBS, the sections were mounted in Mowiol® (Wako, Osaka, Japan) on glass slides. Images were acquired under a laser scanning microscope (FV1200, Olympus, Tokyo, Japan).

Laser Microdissection

Cryosections of cholesteatoma and skin at a thickness of 10 μm were prepared on foil slides (Leica, Wetzlar, Germany). Sections were processed by RNA*later*™ Solution (Invitrogen), stored overnight at −80 °C and then stained with 0.05 % toluidine blue for 1 min. The perimatrix region in each cholesteatoma specimen and the dermal region in each skin sample were identified depending on the positions of the matrix and epidermal regions, and isolated from sections with a LMD7000 laser microdissection system (Leica). RNA was isolated from the fragments using an RNeasy® Micro Kit (Qiagen).

RNA Sequencing and Bioinformatics Analyses

Total RNAs were extracted from cells with an RNeasy® Micro Kit (Qiagen). NGS library preparation was performed using a SMARTer® Stranded Total RNA Sample Prep Kit–Pico Input Mammalian (TaKaRa, Shiga, Japan). Sequencing was performed on an Illumina HiSeq 2500 platform in a 75-base single-end mode. Illumina CASAVA ver. 1.8.2 software was used for basecalling. Sequenced reads were mapped to the human reference genome sequences (hg19) using TopHat v2.0.13 in combination with

Bowtie2 ver. 2.2.3 and SAMtools ver. 0.1.19. The fragments per kilobase of exon per million mapped fragments were calculated using Cuffnorm ver. 2.2.1. The Subio Basic Plug-in (v1.22; Subio Inc.) was used to determine the fold-difference and perform the paired *t* test. Bioinformatics analyses were performed using the PANTHER Classification System (http://www.pantherdb.org/) for functional annotation and Ingenuity Pathway Analysis (Qiagen, http://www.ingenuity.com) for upstream regulator analysis. The raw data have been deposited in the NCBI Gene Expression Omnibus database (GSE116142). Upstream regulator analysis is useful for defining biological interactions predicted to be upregulated or downregulated based on the expression changes observed in gene sets. Statistical analyses of these predictions were carried out to calculate the activation z-score, which is designed to ensure that gene sets composed of randomly chosen perturbed genes with random regulatory influences do not on average produce significant results according to the Ingenuity Downstream Effect Analysis whitepaper (http://pages.ingenuity.com/rs/ingenuity/images/0812%20downstream_effects_analysis_whitepaper.pdf).

Enzyme-Linked Immunosorbent Assay

All cholesteatoma and skin samples were weighed and then sonicated by Sonifier 250 (Branson, Danbury, CT) in PBS. For the PGE2 assay, 10 μM of indomethacin was added to the homogenate buffer. The supernatant of centrifuged samples was measured for concentrations of TNF-α, IL-1β, IL-6, and PGE2. For TNF-α, IL-1β, and IL-6 assays, sandwich enzyme-linked immunosorbent assay (ELISA) (human TNF-α uncoated ELISA, human IL-1β uncoated ELISA, and human IL-6 uncoated ELISA, respectively; Invitrogen) was used. For the PGE2 assay, competitive ELISA (PGE2 ELISA Kit, Enzo) was used. The enzyme reaction was measured at an optical density of 405 nm. Standard 4-parameter logistic curves were prepared by plotting the absorbance values.

In Situ Hybridization

We purchased a plasmid containing the whole cDNA sequence of *IL-1β* (IMAGE clone ID 3875593) to obtain RNA probes. An *IL-1β* antisense probe was produced via the cDNA clone digested with EcoRV and T7 polymerase. The antisense probe was 1559 bp, 1522 bp of which was from the *IL-1β* cDNA. An *IL-1β* sense probe was produced via the cDNA clone digested with Apa1 and SP6 polymerase. Both probes were labeled using a DIG RNA labeling kit (Roche, Indianapolis, IN).

Frozen sections at a thickness of 5 μm were fixed in 4 % PFA in PBS at room temperature for 10 min and immersed in 0.2 M HCl at room temperature for 10 min. Subsequently, they were treated in 4.2 μg/ml proteinase K in PBS at 37 °C for 5 min. The samples were immersed in 0.1 M triethanolamine pH 8.0, followed by acetylation with 0.25 % deionized formamide, 25 % 20× saline sodium citrate (SSC), 200 μg/ml yeast tRNA, and 25 % dH2O. Unbound probes were washed with a descending SSC series, followed by blocking for 1 h at room temperature with 1 % blocking buffer (Blocking Reagent, Roche) in PBS. Slides were incubated at room temperature for 1 h at a 1:1000 dilution of anti-digoxigenin-alkaline phosphatase (Roche Diagnostics, Germany) in 1 % blocking buffer. Samples were reacted overnight at room temperature with nitro blue phosphate/5-bromo,4-chloro, 3-indolil phosphate (Roche) in a detection buffer containing 0.1 M Tris-HCl, 0.1 M NaCl, and 0.05 M $MgCl_2$. Slides were mounted in Fluoromount (Cosmo Bio, Tokyo, Japan) and viewed under an OLYMPAS DP80 microscope.

Statistical Analysis

All data in the figures are displayed as mean ± standard error of mean values, and the Wilcoxon signed rank test was performed to assess statistical significance between two groups, using GraphPad Prism® version 7 (GraphPad Software, La Jolla, CA, USA). $P < 0.05$ was considered significant.

RESULTS

More Osteoclasts Are Seen on the Bone Surface Adjacent to Cholesteatomas than in Non-Lesional Areas

Twenty-four specimens collected from patients who underwent tympanomastoidectomy were assessed in this analysis. In each patient, fragments of temporal bone far from cholesteatoma lesions were collected as controls. To investigate the existence of osteoclasts on the bone surface adjacent to cholesteatomas, we used TRAP staining. TRAP-positive polynuclear osteoclasts were seen on the bone surface adjoining each cholesteatoma (Fig. 1a, b). The number of osteoclasts per μm^2 on the bone surface adjacent to cholesteatomas was significantly larger (Wilcoxon signed-rank test, $p = 0.0203$) than on the surface of control bone (Fig. 1c).

Expression of Receptor Activator of NF-κB Ligand mRNA Is Higher in Cholesteatomas than in Normal Skin

To confirm that osteoclasts were differentiated and activated in the cholesteatoma microenvironment, we

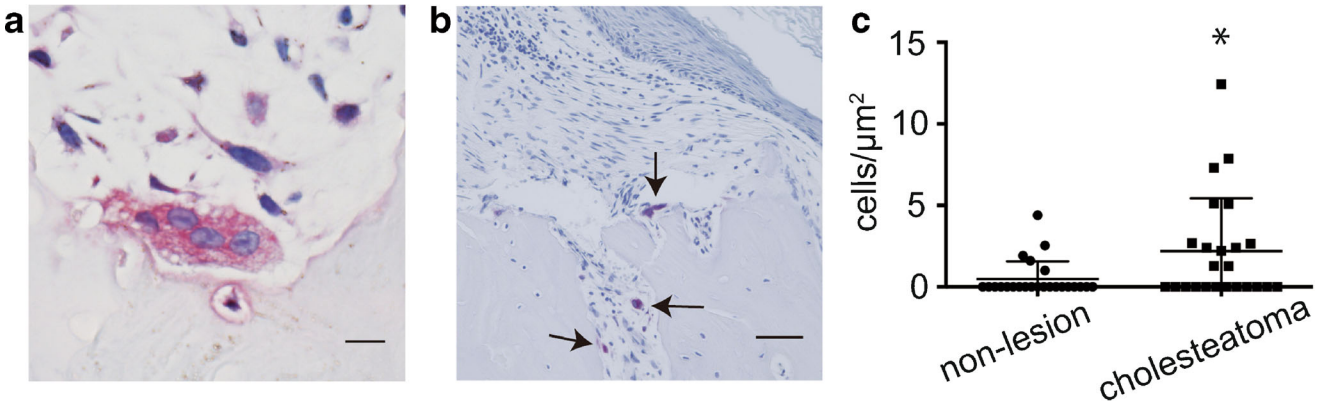

FIG. 1. Elevated numbers of osteoclasts are present on the bone surface adjacent to cholesteatoma lesions. **a** Osteoclast cytoplasm is stained red using TRAP (scale bar: 10 μm). Multiple nuclei are stained blue. **b** Osteoclasts (arrows) are observed on the bone surface adjacent to cholesteatoma lesions (scale bar 50 μm). **c** The number of osteoclasts per μm^2 on the bone surface adjacent to cholesteatoma lesions was larger than those on the surface of non-cholesteatomatous bone ($N = 24$). The asterisk indicates a statistically significant difference

measured the expression of *RANKL* mRNA. RANKL is an essential factor for the differentiation and activation of osteoclasts (Takayanagi 2007). ddPCR was used to quantify *RANKL* mRNA expression both in cholesteatoma samples and in the retroauricular skin as a control. The expression of *RANKL* mRNA corrected by *GAPDH* mRNA was significantly higher in cholesteatomas ($n = 9$) than in control skin (Wilcoxon signed-rank test, $p = 0.0273$) (Fig. 2a).

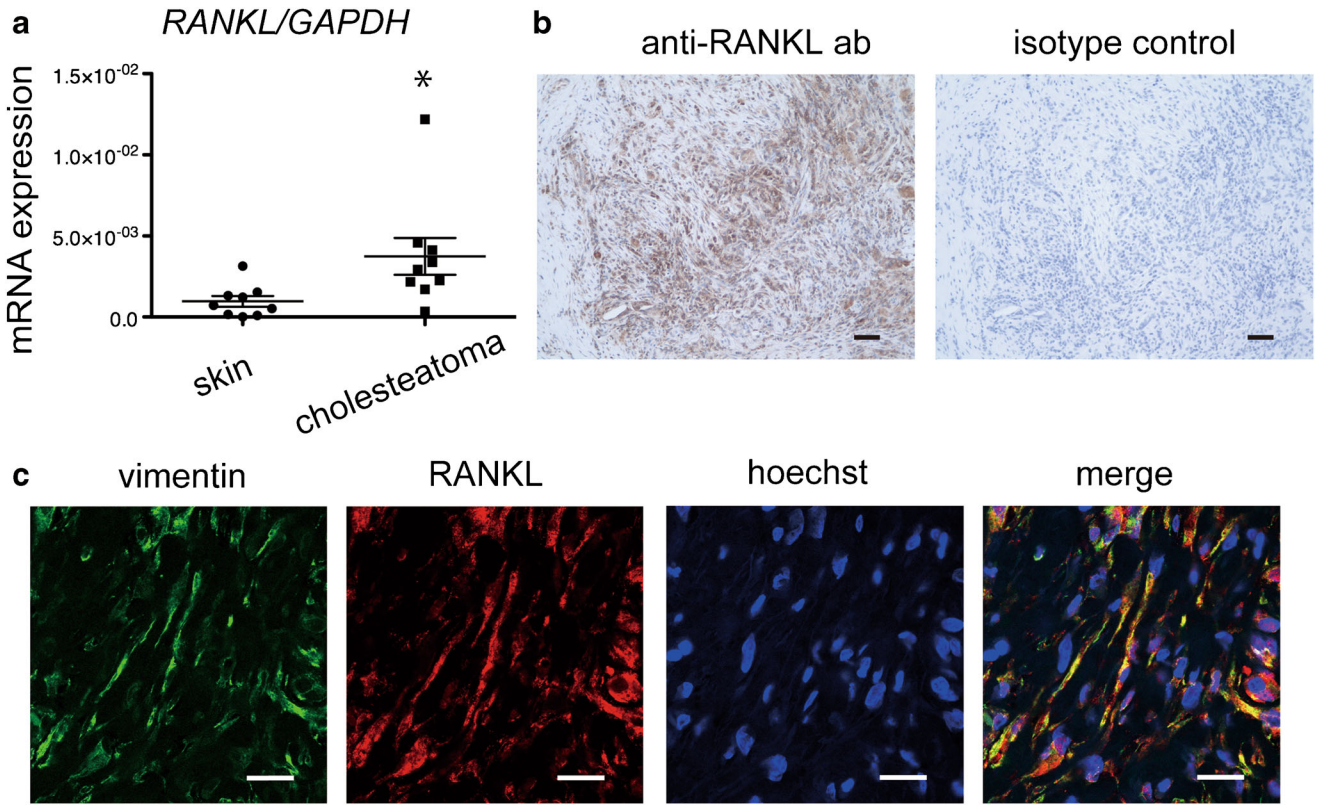

FIG. 2. Fibroblasts in the cholesteatoma perimatrix express RANKL. **a** Expression of *RANKL* mRNA in cholesteatoma, corrected for *GAPDH* mRNA, is significantly higher than in control skin ($n = 9$). The asterisk indicates a statistically significant difference. **b** DAB staining for RANKL in the cholesteatoma perimatrix, counterstained with hematoxylin (scale bars 50 μm). **c** Immunofluorescent staining of the cholesteatoma perimatrix. Co-localization of vimentin and RANKL immunofluorescence shows that fibroblasts in the perimatrix express RANKL. RANKL was labeled with Alexa Fluor® 555, and vimentin was labeled with Alexa Fluor® 488. Nuclei were stained with Hoechst® 33342 (scale bars: 10 μm)

Fibroblasts in Cholesteatomas Express Receptor Activator of NF-κB Ligand

To identify the cellular source of RANKL expression, cholesteatoma sections were subjected to immunohistochemical analysis. RANKL-positive cells with spindle shapes were seen in the cholesteatoma perimatrix on DAB-stained slides (Fig. 2b). Furthermore, double immunofluorescent staining showed co-expression of vimentin and RANKL, indicating that RANKL was expressed in fibroblasts in the cholesteatoma perimatrix (Fig. 2c).

RNA Sequencing and Gene Ontology Analysis Show that the Cholesteatoma Microenvironment Is Suitable for Osteoclast Differentiation and Activation

One sample each of cholesteatoma perimatrix and retroauricular dermis were derived from six patients and dissected out by laser microdissection as shown in Fig. 3a. The fragments underwent RNA sequencing to generate transcriptome profiles (Table S1). RNA sequencing showed that the average of expression levels of *RANKL* mRNA in the cholesteatoma perimatrix was 4.54-fold higher than those in the dermis. The expression levels of 1423 transcripts differed by at least 2-fold (paired t test, $p<0.05$) between the cholesteatoma perimatrix and dermis (Table S2). Referring to the public data of 69 periodontitis patients (Demmer et al. 2008), we found marked similarities in the gene-expression profiles of the cholesteatoma perimatrix and gingival tissue with periodontitis by NextBio analysis (Fig. 3b). To investigate the relationship between cholesteatoma and osteoclast differentiation, these mRNAs were subjected to gene ontology (GO) analysis using the PANTHER™ Classification System (http://www.pantherdb.org/). GO analysis revealed that expression levels of this gene set (GO: 0045780, GO term: positive regulation of bone resorption) were significantly higher (PANTHER™ Overrepresentation Test released March 8, 2019; $p=0.0194$) in the cholesteatoma perimatrix than in the dermis.

Ingenuity Pathway Analysis and Upstream Analysis Identify Candidate Transcription Factors that Regulate Receptor Activator of NF-κB Ligand Expression

We used Ingenuity Pathway Analysis (IPA), a technique that identifies candidate biomarkers in the context of biological systems, to investigate which factors control RANKL expression in the cholesteatoma perimatrix. Causal Network Analysis, a component of IPA, reveals causal relationships associated with experimental data. mRNAs with at least a 2-fold absolute difference (paired t test, $p<0.05$) between the cholesteatoma perimatrix and dermis were used for IPA. Sixty-two candidate transcription

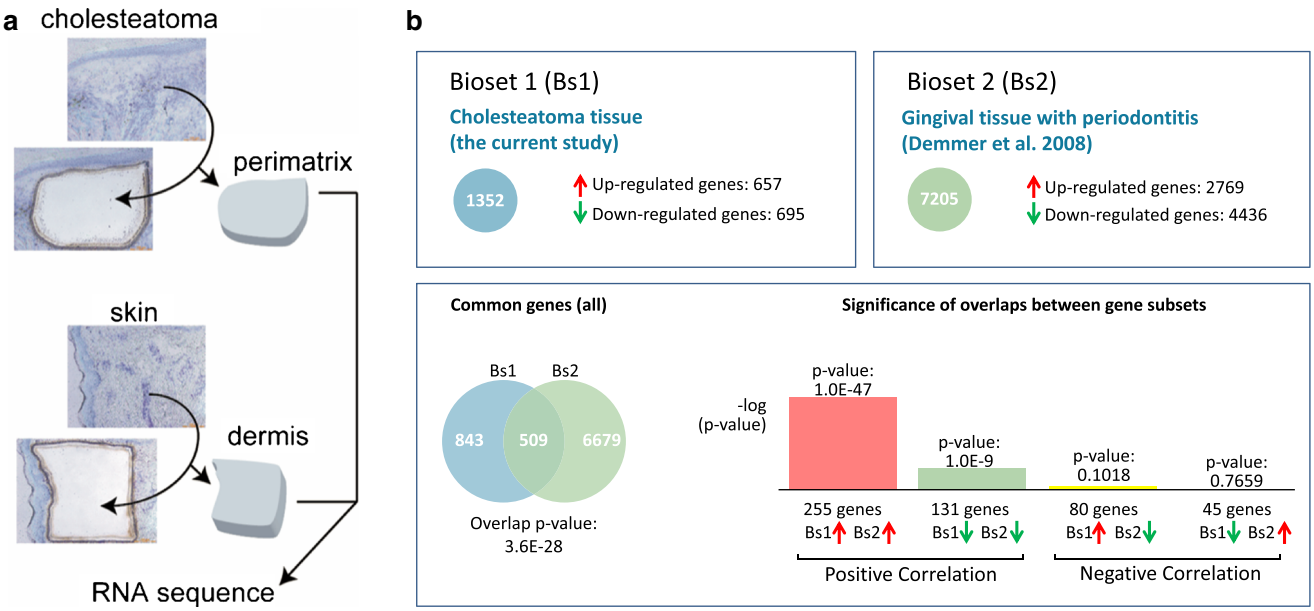

FIG. 3. Osteoclast differentiation is positively regulated in the cholesteatoma perimatrix. **a** Illustration of the technique used to dissect the perimatrix and dermis from the cholesteatoma and skin by laser microdissection. **b** Significance of the overlap between gene sets of cholesteatoma tissue and gingival tissue with periodontitis. The scale of the bars is measured in -log (P value). The accession number for the public data used for the graphs is GE16134

factors upstream of RANKL were identified in the cholesteatoma perimatrix (Table 1). Candidates with IPA-derived z-scores over 2 were considered significantly activated.

The Concentrations of IL-1β, IL-6, TNF-α, and PGE2 in Cholesteatomas Are Higher than Those in the Skin

Among the candidate upstream transcription factors for RANKL identified by IPA, IL-1β, IL-6, TNF-α, and PGE2 are inflammatory cytokines or chemical mediators considered to be related to bone destruction by osteoclasts (Akaogi et al. 2006; Kim et al. 2014; Kim et al. 2007). We measured protein levels of these candidates by ELISA. The actual concentrations of IL-1β, IL-6, TNF-α, and PGE2 in cholesteatomas were significantly higher (Wilcoxon signed-rank test, $p = 0.0137$, 0.0234, 0.0215, and 0.0186, respectively) than those in the skin (Fig. 4a–d). In situ hybridization showed that mononuclear infiltrating cells in the cholesteatoma perimatrix expressed *IL-1β* mRNA. Keratinocytes in the matrix and fibroblasts in the perimatrix of cholesteatomas did not express *IL-1β* mRNA (Fig. 4e).

DISCUSSION

In cholesteatoma, it remains unclear whether osteoclasts are differentiated and activated and whether they are involved in bone erosion. Bone remodeling, a continuous process involving bone resorption by osteoclasts and bone formation by osteoblasts, is needed to repair damaged bones and maintain mineral homeostasis (Raggatt and Partridge 2010). Osteoclastic resorption has been reported in the human temporal bone without inflammation or bone disease (Kamakura and Nadol 2017). It is therefore important and necessary to compare osteoclasts derived under pathologic and physiological conditions. Prior to this study, there was no published information regarding the number of osteoclasts per unit area on normal temporal bone, so here, we defined control bone as non-diseased temporal bone in patients with cholesteatoma. Histological examination by TRAP staining demonstrated a larger number of osteoclasts on the bone surface adjacent to cholesteatomas than on control bone, suggesting that osteoclasts were differentiated and activated in cholesteatoma and played an important role in bone erosion. The number of osteoclasts per unit area was proportional to the degree of cholesteatoma invasion, but this relationship was not significant (data not shown).

Osteoclast differentiation and activation are regulated by RANKL and M-CSF (Boyle et al. 2003). In bone disease with inflammation, such as that characterizing RA or periodontitis, RANKL-

TABLE 1

Sixty-two candidate upstream transcription factors for RANKL expression in the cholesteatoma perimatrix

Activation z-score		*Activation z-score*	
Lipopolysaccharide	8.866	NfkB1-RelA	3.25
TNF	8.427	ITGB1	3.25
IL1B	7.446	ATF4	3.241
IL6	6.703	IL18	3.229
NFkB (complex)	6.43	Lipoteichoic acid	3.218
IFNG	6.107	ANGPT2	3.16
CD28	6.054	Tnf (family)	3.153
TGFB1	5.824	SPP1	3.051
CD3	5.731	IL1A	5.612
OSM	5.501	IL32	2.927
Doxorubicin	5.33	ATP	2.857
E. coli B5 lipopolysaccharide	5.259	miR-1227-5p	2.849
MYD88	5.197	SP1	2.834
IL1	4.974	MAPK3	2.819
cytokine	4.83	AKT1	2.78
TLR4	4.821	Ca2+	2.72
Hydrogen peroxide	4.8	LIF	2.694
P38 MAPK	4.762	Isoproterenol	2.675
IL17A	4.553	ADRB2	2.621
TNFSF11	4.527	NFATC1	2.611
IL2	4.462	PTH	2.609
IL15	4.455	miR-6795-3p	2.605
STAT1	4.429	CEBPD	2.601
miR-6762-5p	4.335	miR-3070-5p	2.592
AGT	4.332	PRL	2.584
CREB1	4.239	Beta-estradiol	2.582
Tretinoin	4.234	PLG	2.582
TICAM1	4.141	Bucladesine	2.487
miR-7113-5p	4.058	Ethanol	2.463
TCR	4.029	IL23	2.416
STAT3	4.019	TNC	2.376
Prostaglandin E2	4.01	ITGA9	2.371
miR-128-1-5p	3.964	RUNX2	2.302
PTGS2	3.958	miR-4749-3p	2.278
CD40LG	3.927	miR-1915-3p	2.269
FGF2	3.896	VitaminD3-VDR-RXR	2.261
IL7	3.886	Histamine	2.259
IL21	3.847	PGR	2.254
HMGB1	3.793	NCR2	2.236
CEBPB	3.608	Stat3-Stat3	2.219
Reactive oxygen species	3.602	Sphingosine-1-phosphate	2.198
Ionomycin	3.585	ADAM17	2.189
XBP1	3.541	FOS	2.183
EGR1	3.518	miR-6887-3p	2.152
IL27	3.481	LEP	2.131
IL33	3.456	CXCL12	2.062
IL6R	3.294	IL4	2.059
NOD2	3.293	miR-5104b-5p	2.023

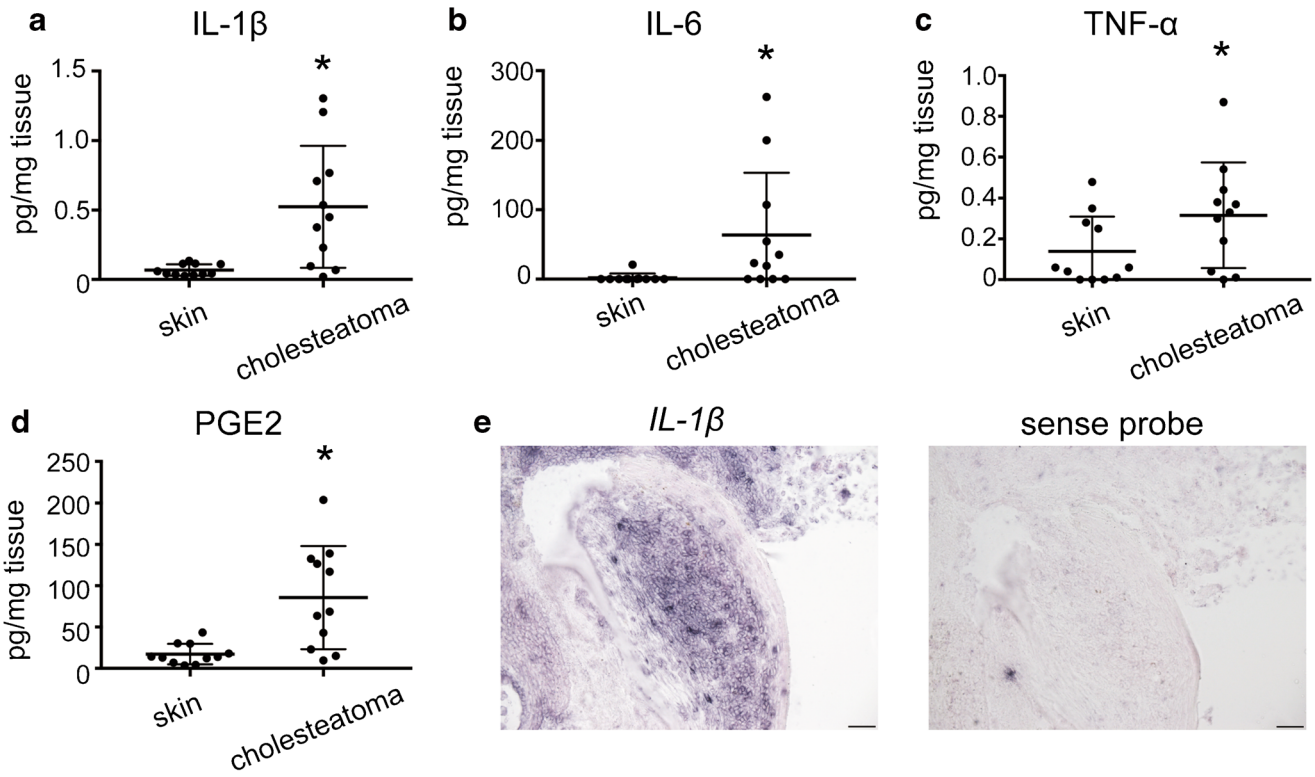

FIG. 4. Concentrations of IL-1β, IL-6, TNF-α, and PGE2 in cholesteatomas. **a–d** ELISA measurements show that the concentrations of IL-1β, IL-6, TNF-α, and PGE2 are higher in cholesteatoma than in skin ($n = 11$). The asterisks indicate statistically significant differences. **e** Mononuclear infiltrating cells in the cholesteatoma perimatrix express *IL-1β* mRNA, as shown in the left panel using in situ hybridization. The right panel shows in situ hybridization using a sense probe as a negative control (scale bars 50 μm)

mediated osteoclastogenesis plays an important role in bone destruction (Hienz et al. 2015; McInnes and Schett 2011). However, it remains controversial whether cholesteatoma expresses RANKL (Chen et al. 2015; Jeong et al. 2006; Koizumi et al. 2016; Kuczkowski et al. 2010). In the current study, ddPCR and RNA sequencing demonstrated that the expression of *RANKL* mRNA in human cholesteatoma samples was higher than that in retroauricular skin, suggesting that osteoclasts in cholesteatoma were activated by RANKL. With regard to the origin of RANKL, immunofluorescent staining of cholesteatoma samples showed vimentin-positive, spindle-shaped cells in the perimatrix that were considered to be fibroblasts expressing RANKL. This finding supports the results of our previous study, in which fibroblasts surrounding the epithelial lamina expressed RANKL in both a mouse model and an in vitro culture system (Iwamoto et al. 2016).

We further investigated the gene profile of the perimatrix by RNA sequencing, which can provide comprehensive information regarding the gene expression of mRNAs. Using GO analysis, RNA sequencing results can be functionally interpreted via enrichment analysis. Given a set of genes that are upregulated under certain conditions, GO term enrichment analysis can determine which GO terms are over- or under-represented by using annotations for that gene set (Ashburner et al. 2000). In addition, IPA is a powerful analysis and search tool that can identify new targets or candidate biomarkers within the context of biological systems. IPA Upstream Regulator analysis makes it possible to identify the cascade of upstream transcription factors responsible for gene expression changes in a dataset, and to illuminate the biological activities occurring in both diseased and non-diseased tissues. These candidate transcription factors include cytokines, growth factors, miRNAs, drugs, and chemicals (https://www.qiagenbioinformatics.com/) (Kramer et al. 2014). In the current study, RNA sequencing revealed that *RANKL* mRNA was more highly expressed in the cholesteatoma perimatrix than in

the dermis in samples. The GO term "positive regulation of bone resorption" was significantly over-represented, indicating that the microenvironment of the cholesteatoma perimatrix promoted bone resorption. Positive correlation with gingival tissue with periodontitis revealed by NextBio analysis indicated that the pathology of cholesteatoma was similar with that of periodontitis which was a degenerative bone disease.

Using IPA analysis, we identified candidate transcription factors upstream of RANKL. These included lipopolysaccharide (LPS), pre-inflammatory cytokines, and other mediators (Table 1), which is consistent with the theory that these substances lead to bone destruction (Si et al. 2015). LPS, directly and/or indirectly, may upregulate RANKL expression in the cholesteatoma perimatrix.

We investigated whether cholesteatomas contained transcription regulators that would induce the cholesteatoma perimatrix to express RANKL. ELISA revealed that the concentrations of IL-1β, IL-6, TNF-α, and PGE2 in cholesteatomas were higher than those in the skin. These compounds are well known to be major contributors to osteoclastogenesis in RA and periodontitis. In particular, the IL-1 family is abundantly expressed in RA and promotes osteoclast activation (McInnes and Schett 2007). Thus, a similar pathway leading to osteoclast activation is suggested to occur in cholesteatoma.

A monoclonal anti-TNF-α antibody was reported to attenuate the progression of joint damage in patients with RA and has been widely used in RA treatment (Lipsky et al. 2000). An IL-1 receptor antagonist and an anti-IL-6 receptor antibody were also reported to reduce arthritis symptoms in patients with RA (Bresnihan et al. 1998; Choy et al. 2002). These molecular-targeted agents may suppress signaling from the upstream molecules identified in the current study and inhibit bone erosion in cholesteatoma. The current study proposes the possibility of non-surgical treatment for preventing bone erosion in cholesteatoma and provides a strategy for formulating ear drop solutions that contain either these molecular-targeted agents or cyclooxygenase-2 inhibitors, which reduce PGE2 production. Further studies will be needed to evaluate the effectiveness and adverse reactions of these agents.

ACKNOWLEDGMENTS

We would like to thank Dr. Hiroyuki Murota, Dr. Mari Kaneda, Dr. Saori Ochi, Dr. Takefumi Kamakura, and Dr. Yohei Maeda for the helpful discussions, and Ms. Yumiko Fujii and Ms. Sayaka Matsumura for research assistance.

Funding information This work was supported by a JSPS KAKENHI Grant (nos. JP16K20242).

COMPLIANCE WITH ETHICAL STANDARDS

Conflict of Interest The authors declare that they have no conflicts of interest.

REFERENCES

Abramson M, Moriyama H, Huang CC (1984) Pathogenic factors in bone resorption in cholesteatoma. Acta Otolaryngol 97:437–442. https://doi.org/10.3109/00016488409132918

Akaogi J, Nozaki T, Satoh M, Yamada H (2006) Role of PGE2 and EP receptors in the pathogenesis of rheumatoid arthritis and as a novel therapeutic strategy endocrine. Metab Immune Disord Drug Targets 6:383–394. https://doi.org/10.2174/187153006779025711

Ashburner M, Ball CA, Blake JA, Botstein D, Butler H, Cherry JM, Davis AP, Dolinski K, Dwight SS, Eppig JT, Harris MA, Hill DP, Issel-Tarver L, Kasarskis A, Lewis S, Matese JC, Richardson JE, Ringwald M, Rubin GM, Sherlock G (2000) Gene ontology: tool for the unification of biology. The Gene Ontology Consortium. Nat Genet 25:25–29. https://doi.org/10.1038/75556

Boyle WJ, Simonet WS, Lacey DL (2003) Osteoclast differentiation and activation. Nature 423:337–342. https://doi.org/10.1038/nature01658

Bresnihan B et al (1998) Treatment of rheumatoid arthritis with recombinant human interleukin-1 receptor antagonist. Arthritis Rheum 41:2196–2204. https://doi.org/10.1002/1529-0131(199812)41:12<2196::Aid-art15>3.0.Co;2-2

Chen AP et al (2015) Expression levels of receptor activator of nuclear factor-kappaB ligand and osteoprotegerin are associated with middle ear cholesteatoma risk. Acta Otolaryngol 135:655–666. https://doi.org/10.3109/00016489.2015.1011789

Cheshire IM, Blight A, Ratcliffe WA, Proops DW, Heath DA (1991) Production of parathyroid-hormone-related protein by cholesteatoma cells in culture. Lancet 338:1041–1043

Chi Z, Wang Z, Liang Q, Zhu Y, du Q (2015) Induction of cytokine production in cholesteatoma keratinocytes by extracellular high-mobility group box chromosomal protein 1 combined with DNA released by apoptotic cholesteatoma keratinocytes. Mol Cell Biochem 400:189–200. https://doi.org/10.1007/s11010-014-2275-0

Chole RA (1984) Cellular and subcellular events of bone resorption in human and experimental cholesteatoma: the role of osteoclasts. Laryngoscope 94:76–95

Choy EH et al (2002) Therapeutic benefit of blocking interleukin-6 activity with an anti-interleukin-6 receptor monoclonal antibody in rheumatoid arthritis: a randomized, double-blind, placebo-controlled, dose-escalation trial. Arthritis Rheum 46:3143–3150. https://doi.org/10.1002/art.10623

COCHRAN DL (2008) Inflammation and bone loss in periodontal disease. J Periodontol 79:1569–1576. https://doi.org/10.1902/jop.2008.080233

DEMMER RT ET AL (2008) Transcriptomes in healthy and diseased gingival tissues. J Periodontol 79:2112–2124. https://doi.org/10.1902/jop.2008.080139

FUJIHARA R ET AL (2014) Tumor necrosis factor-alpha enhances RANKL expression in gingival epithelial cells via protein kinase a signaling. J Periodontal Res 49:508–517. https://doi.org/10.1111/jre.12131

HAMZEI M ET AL (2003) Osteoclast stimulating and differentiating factors in human cholesteatoma. Laryngoscope 113:436–442. https://doi.org/10.1097/00005537-200303000-00009

HIENZ SA, PALIWAL S, IVANOVSKI S (2015) Mechanisms of bone resorption in periodontitis. J Immunol Res 2015:615486. https://doi.org/10.1155/2015/615486

HUANG CC, YI ZX, YUAN QG, ABRAMSON M (1990) A morphometric study of the effects of pressure on bone resorption in the middle ear of rats. Am J Otolaryngol 11:39–43

IINO Y, HOSHINO E, TOMIOKA S, TAKASAKA T, KANEKO Y, YUASA R (1983) Organic acids and anaerobic microorganisms in the contents of the cholesteatoma sac. Ann Otol Rhinol Laryngol 92:91–96. https://doi.org/10.1177/000348948309200122

IWAMOTO Y ET AL (2016) Intercellular communication between keratinocytes and fibroblasts induces local osteoclast differentiation: a mechanism underlying cholesteatoma-induced bone destruction. Mol Cell Biol 36:1610–1620. https://doi.org/10.1128/MCB.01028-15

JEONG JH, PARK CW, TAE K, LEE SH, SHIN DH, KIM KR, PARK YW (2006) Expression of RANKL and OPG in middle ear cholesteatoma tissue. Laryngoscope 116:1180–1184. https://doi.org/10.1097/01.mlg.0000224345.59291.da

JUNG TT, JUHN SK (1988) Prostaglandins in human cholesteatoma and granulation tissue. Am J Otolaryngol 9:197–200

JUNG JY, PASHIA ME, NISHIMOTO SY, FADDIS BT, CHOLE RA (2004) A possible role for nitric oxide in osteoclastogenesis associated with cholesteatoma. Otol Neurotol 25:661–668

KAMAKURA T, NADOL JB JR (2017) Evidence of osteoclastic activity in the human temporal bone. Audiol Neurootol 22:218–225. https://doi.org/10.1159/000481279

KIM KW ET AL (2007) Human rheumatoid synovial fibroblasts promote osteoclastogenic activity by activating RANKL via TLR-2 and TLR-4 activation. Immunol Lett 110:54–64. https://doi.org/10.1016/j.imlet.2007.03.004

KIM HR, KIM KW, KIM BM, JUNG HG, CHO ML, LEE SH (2014) Reciprocal activation of CD4+ T cells and synovial fibroblasts by stromal cell-derived factor 1 promotes RANKL expression and osteoclastogenesis in rheumatoid arthritis. Arthritis Rheum 66:538–548. https://doi.org/10.1002/art.38286

KOBAYASHI H, ASANO K, KANAI K, SUZAKI H (2005) Suppressive activity of vitamin D3 on matrix metalloproteinase production from cholesteatoma keratinocytes in vitro. Mediat Inflamm 2005:210–215. https://doi.org/10.1155/MI.2005.210

KOIZUMI H, SUZUKI H, OHBUCHI T, KITAMURA T, HASHIDA K, NAKAMURA M (2015) Increased permeability of the epithelium of middle ear cholesteatoma. Clin Otolaryngol 40:106–114. https://doi.org/10.1111/coa.12332

KOIZUMI H, SUZUKI H, IKEZAKI S, OHBUCHI T, HASHIDA K, SAKAI A (2016) Osteoclasts are not activated in middle ear cholesteatoma. J Bone Miner Metab 34:193–200. https://doi.org/10.1007/s00774-015-0655-5

KOIZUMI H ET AL (2017) Presence of osteoclasts in middle ear cholesteatoma: a study of undecalcified bone sections. Acta Otolaryngol 137:127–130. https://doi.org/10.1080/00016489.2016.1222549

KRAMER A, GREEN J, POLLARD J JR, TUGENDREICH S (2014) Causal analysis approaches in Ingenuity Pathway Analysis. Bioinformatics 30:523–530. https://doi.org/10.1093/bioinformatics/btt703

KUCZKOWSKI J, KOBIERSKA-GULIDA G, IZYCKA-SWIESZEWSKA E, POTOCKA M, MIKASZEWSKI B, SIERSZEN W (2010) Molecular control of bone resorption in chronic otitis media with cholesteatoma. Otolaryngol Pol 64:219–224. https://doi.org/10.1016/S0030-6657(10)70019-6

KUCZKOWSKI J, SAKOWICZ-BURKIEWICZ M, IZYCKA-SWIESZEWSKA E, MIKASZEWSKI B, PAWELCZYK T (2011) Expression of tumor necrosis factor-alpha, interleukin-1alpha, interleukin-6 and interleukin-10 in chronic otitis media with bone osteolysis ORL. J Otorhinolaryngol Relat Spec 73:93–99. https://doi.org/10.1159/000323831

KUO CL, SHIAO AS, YUNG M, SAKAGAMI M, SUDHOFF H, WANG CH, HSU CH, LIEN CF (2015) Updates and knowledge gaps in cholesteatoma research. Biomed Res Int 2015:854024–854017. https://doi.org/10.1155/2015/854024

LIKUS W ET AL (2016) Bacterial infections and osteoclastogenesis regulators in men and women with cholesteatoma arch. Immunol Ther Exp (Warsz) 64:241–247. https://doi.org/10.1007/s00005-015-0373-7

LIPSKY PE, VAN DER HEIJDE D, ST CLAIR EW, FURST DE, BREEDVELD FC, KALDEN JR, SMOLEN JS, WEISMAN M, EMERY P, FELDMANN M, HARRIMAN GR, MAINI RN, ANTI-TUMOR NECROSIS FACTOR TRIAL IN RHEUMATOID ARTHRITIS WITH CONCOMITANT THERAPY STUDY GROUP (2000) Infliximab and methotrexate in the treatment of rheumatoid arthritis. N Engl J Med 343:1594–1602. https://doi.org/10.1056/NEJM200011303432202

MCINNES IB, SCHETT G (2007) Cytokines in the pathogenesis of rheumatoid arthritis. Nat Rev Immunol 7:429–442. https://doi.org/10.1038/nri2094

MCINNES IB, SCHETT G (2011) The pathogenesis of rheumatoid arthritis. N Engl J Med 365:2205–2219. https://doi.org/10.1056/NEJMra1004965

OLSZEWSKA E, WAGNER M, BERNAL-SPREKELSEN M, EBMEYER J, DAZERT S, HILDMANN H, SUDHOFF H (2004) Etiopathogenesis of cholesteatoma. Eur Arch Otorhinolaryngol 261:6–24. https://doi.org/10.1007/s00405-003-0623-x

PEEK FA, HUISMAN MA, BERCKMANS RJ, STURK A, VAN LOON J, GROTE JJ (2003) Lipopolysaccharide concentration and bone resorption in cholesteatoma. Otol Neurotol 24:709–713

RAGGATT LJ, PARTRIDGE NC (2010) Cellular and molecular mechanisms of bone remodeling. J Biol Chem 285:25103–25108. https://doi.org/10.1074/jbc.R109.041087

REHMAN MT, HOYLAND JA, DENTON J, FREEMONT AJ (1994) Age related histomorphometric changes in bone in normal British men and women. J Clin Pathol 47:529–534

RITCHLIN CT, HAAS-SMITH SA, LI P, HICKS DG, SCHWARZ EM (2003) Mechanisms of TNF-α– and RANKL-mediated osteoclastogenesis and bone resorption in psoriatic arthritis. J Clin Investig 111:821–831. https://doi.org/10.1172/jci200316069

SATO K, SUEMATSU A, OKAMOTO K, YAMAGUCHI A, MORISHITA Y, KADONO Y, TANAKA S, KODAMA T, AKIRA S, IWAKURA Y, CUA DJ, TAKAYANAGI H (2006) Th17 functions as an osteoclastogenic helper T cell subset that links T cell activation and bone destruction. J Exp Med 203:2673–2682. https://doi.org/10.1084/jem.20061775

SI Y ET AL (2015) TLR4 drives the pathogenesis of acquired cholesteatoma by promoting local inflammation and bone destruction. Sci Rep 5:16683. https://doi.org/10.1038/srep16683

TAKAYANAGI H (2007) Osteoimmunology: shared mechanisms and crosstalk between the immune and bone systems. Nat Rev Immunol 7:292–304. https://doi.org/10.1038/nri2062

TAKAYANAGI H ET AL (2000) Involvement of receptor activator of nuclear factor kappa B ligand/osteoclast differentiation factor in osteoclastogenesis from synoviocytes in rheumatoid arthritis.

Arthritis Rheum 43:259–269. https://doi.org/10.1002/1529-0131(200002)43:2<259::Aid-Anr4>3.0.Co;2-W

Teitelbaum SL, Ross FP (2003) Genetic regulation of osteoclast development and function. Nat Rev Genet 4:638–649. https://doi.org/10.1038/nrg1122

Tomlin J, Chang D, McCutcheon B, Harris J (2013) Surgical technique and recurrence in cholesteatoma: a meta-analysis. Audiol Neurootol 18:135–142. https://doi.org/10.1159/000346140

Uno Y, Saito R (1995) Bone resorption in human cholesteatoma: morphological study with scanning electron microscopy. Ann Otol Rhinol Laryngol 104:463–468. https://doi.org/10.1177/000348949510400609

Vitale RF, Ribeiro Fde A (2007) The role of tumor necrosis factor-alpha (TNF-alpha) in bone resorption present in middle ear cholesteatoma. Braz J Otorhinolaryngol 73:117–121. https://doi.org/10.1016/S1808-8694(15)31133-2

Xie S, Xiang Y, Wang X, Ren H, Yin T, Ren J, Liu W (2016) Acquired cholesteatoma epithelial hyperproliferation: roles of cell proliferation signal pathways. Laryngoscope 126:1923–1930. https://doi.org/10.1002/lary.25834

Yetiser S, Satar B, Aydin N (2002) Expression of epidermal growth factor, tumor necrosis factor-α, and interleukin-1α in chronic otitis media with or without cholesteatoma. Otol Neurotol 23:647–652. https://doi.org/10.1097/00129492-200209000-00007